Jean-Marie Lauenstein

Recent Radiation Test Results for Trench Power MOSFETs

Jean-Marie Lauenstein[1], Megan Casey[1], Edward Wilcox[2], Anthony Phan[2], Hak Kim[2], Alyson Topper[2], Ray Ladbury[1], and Ken LaBel[1]

1. NASA Goddard Space Flight Center, Greenbelt, MD; 2. AS&D, Inc., Beltsville, MD

National Aeronautics and Space Administration

Abstract: Single-event effect (SEE) test results are presented for commercial grade, automotive grade, and radiation-hardened trench power MOSFETs.

Introduction

This work presents heavy-ion and proton test data for various trench-gate power metal-oxide-semiconductor field-effect transistors (MOSFETs) (see **Table I**). Devices evaluated include the first (and only) radiation-hardened trench-gate power MOSFET, as well as n-type commercial and both n- and p-type automotive-grade MOSFETs. Typically, safe-operating areas for single-event effects (SEE) in power MOSFETs are established using ions with atomic number (Z) >35 and high linear energy transfer (LET) (>37 MeV·cm²/mg) to ensure safety in the majority of space radiation environments. In contrast, the objectives of this work were in part to evaluate non-hardened vertical trench-gate power MOSFETs with lower-LET, lighter ions relevant to higher-risk tolerant, shorter-duration space missions such as CubeSATs (see **Table II**).

N-type trench-gate power MOSFETs are vulnerable to both catastrophic SEE and degradation due to localized ionizing dose effects from heavy ions [1-7] (see **Fig. 1**). Degradation of the commercial Si7414DN is explored in this work.

Table I: Summary of Power MOSFETs Tested

Part #	Manufacturer	Grade	BV_{DSS} (V)	I_D (A)	R_{DS_ON} (Ω)
Si7414DN	Vishay	Commercial	60	8.7	0.025
SQS460EN	Vishay	Automotive	60	8	0.036
SQJ431EP	Vishay	Automotive	-200	-12	0.213
NVTFS5116PL	ON Semi	Automotive	-60	14	0.052
BSS84AKV	Nexperia	Automotive	-50	0.17	7.5
IRHLF87Y20	Int'l Rectifier	Rad Hardened	20	12	0.032

*BV_{DSS} = drain-source breakdown voltage; I_D = drain current; R_{DS_ON} = drain-source on-state resistance

Table II: Beam Facilities and Ions Used Values are Surface-Incident to the Die

Facility	Ion Species	Air Gap *(cm)*	Surface Energy *(MeV)*	Surface LET *(MeV·cm²/mg)*	Range *(µm)*
TAMU	^{20}Ne	1.5	283	2.7	279
TAMU	^{40}Ar	1.5	548	8.2	202
LBNL	^{40}Ar	0	400	9.7	130
LBNL	^{65}Cu	0	659	21	108
LBNL	^{86}Kr	0	886	31	110
LBNL	^{107}Ag	0	1039	48	90
MGH	proton	15	200	0.0036	138,120

*LBNL = Lawrence Berkeley National Laboratory; LET = linear energy transfer; MGH = Massachusetts General Hospital; TAMU = Texas A&M University.

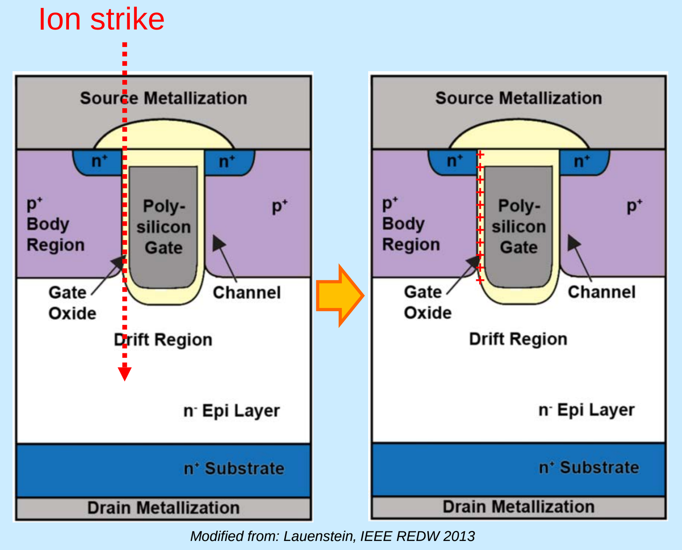

Fig. 1. Illustrative cross section of an n-type trench-gate vertical MOSFET demonstrating how an ion strike through the gate oxide can result in a localized shift in the flat-band voltage, reducing the gate threshold voltage in that location.

Test Methods

Part Preparation

- Decapsulation via acid-etching or manufacturer-supplied unlidded.
- Sample size per ion species: 1-5 pieces

Single-Event Effect Testing

- Test conditions:
  - Gate-source voltage (V_{GS}) held at 0 V (off-state);
    - IRHLF87Y20 also evaluated at V_{GS} = -1 V, -2 V, and -3 V
  - Drain-source voltage (V_{DS}) incremented by ≤ 5% of rated V_{DS} before each run (IRHLF87Y20 incremented by 10%);
  - Post-irradiation gate stress (PIGS) test performed and BV_{DSS} measured after each run.
    - Other optional measurements included: Gate threshold voltage ($V_{GS(th)}$), zero-gate voltage drain leakage current (I_{DSS}), and/or I_D-V_{GS} curves
- Failure criteria:
  - Gate current (I_G) exceeding manufacturer specification during beam run or PIGS test, and/or
  - BV_{DSS} out of manufacturer specification and sudden increase of drain current (I_D) during irradiation

Test Setup

- Heavy Ion Tests (**Figs. 3 – 5**):

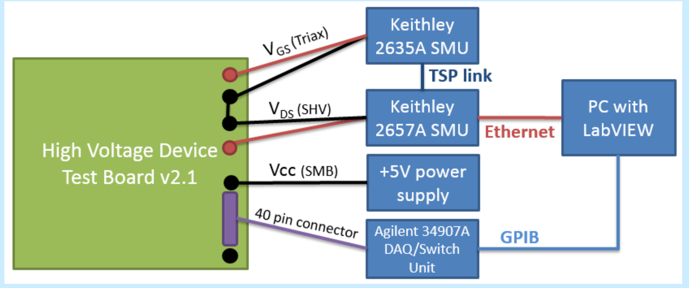

Fig. 3. Block diagram of heavy-ion test setup. Source-measurement units (SMU) included either 2600 series or 2400 series.

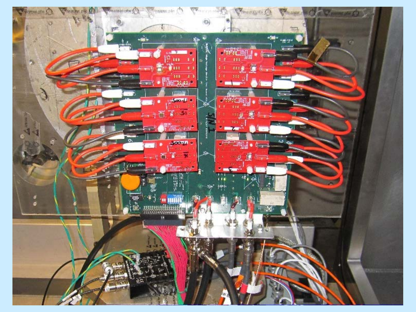

Fig. 4. Test board with 6 daughter cards mounted in vacuum chamber at LBNL.

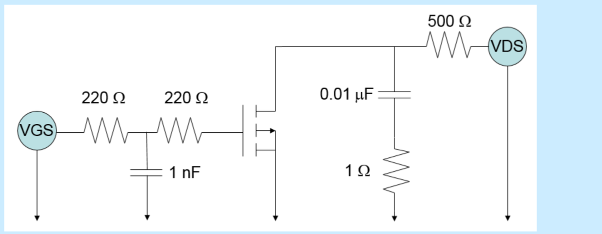

Fig. 5. Equivalent test circuit, compliant with MIL-STD-750 TM1080 [9].

- Proton Tests (**Figs. 6 – 7**):

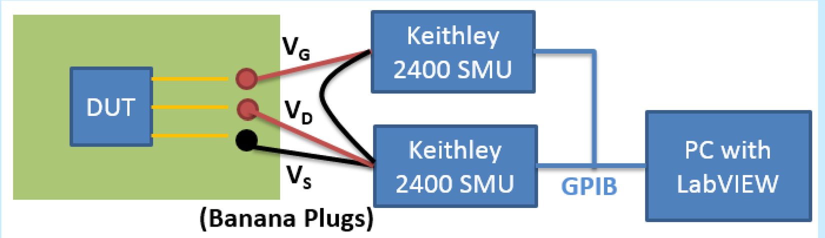

Fig. 6. Block diagram of proton test setup. SMUs connected directly to daughter card on which the device under test (DUT) was mounted.

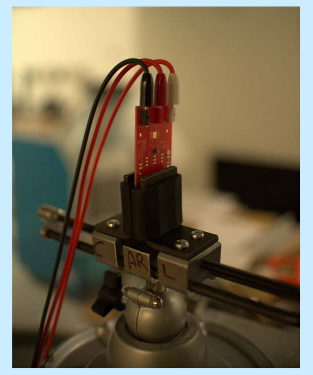

Fig. 7. Daughter card positioned in proton beamline.

Results: N-Type Commercial & Automotive

The Vishay Si7414DN commercial and SQS460DN automotive 60-V MOSFETs differed in susceptibility to single-event burnout (SEB) as a function of ion species & LET (**Figs. 8 – 9**), demonstrating that test results cannot be generalized within a manufacturer. Part-to-part variability occurs in both devices, with the Si7414DN exhibiting possible bimodal behavior (see **Fig 9**, LET = 8.2 MeV·cm²/mg). The Si7414DN remained susceptible to SEB with 283-MeV Ne (LET = 2.7 MeV·cm²/mg). Preliminary 200-MeV proton tests performed without stiffening capacitance (**Fig. 6**) demonstrated drain current spikes (**Fig. 10**) whose onset V_{DS} corresponded to the heavy-ion threshold V_{DS} for SEB, suggesting these may be quenched SEB events.

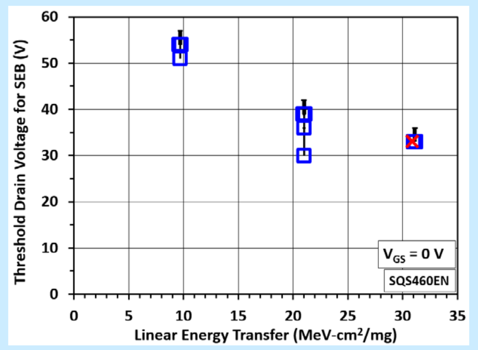

Fig. 8. SQS460EN individual DUT threshold V_{DS} for SEB at 0 V_{GS}. Square markers indicate highest passing V_{DS}; error bars extend to V_{DS} at which SEB occurred. SEB occurred on first beam run for DUT indicated by X marker.

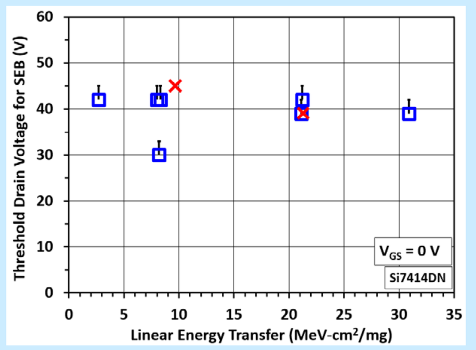

Fig. 9. Si7414DN individual DUT threshold V_{DS} for SEB at 0 V_{GS}. Square markers indicate highest passing V_{DS}; error bars extend to V_{DS} at which SEB occurred. SEB occurred on first beam run for DUTs indicated by X markers.

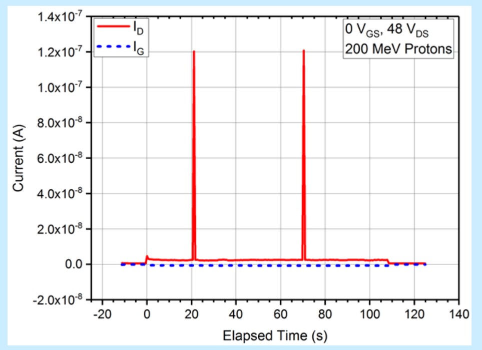

Fig. 10. Si7414DN striptape of drain (red line) and gate (blue dashed line) currents during irradiation with 200 MeV protons at 0 V_{GS} & 48 V_{DS}, showing possible quenched SEB events.

As expected from [1-7], the n-type MOSFETs showed discrete increases in I_D during heavy-ion irradiation (ex/ **Fig. 11**) due to localized dosing of the gate oxide (see **Fig. 1**). Although the SEB events at/just above the SEB threshold V_{DS} did not result in run-away current (ex/ **Fig. 12**), SEB is distinguishable by the magnitude of the event during the run and analysis of the post-rad BV_{DSS} curve (**Fig. 13**). Dose effects resulted in increased leakage I_D but had little or no effect on the breakdown voltage. After SEB, the BV_{DSS} curve is very different and the leakage I_D at 0 V_{GS} remains unchanged when measured at the maximum -20 V_{GS} off-state bias (**Fig. 13**).

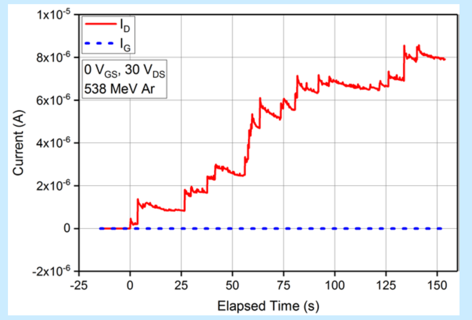

Fig. 11. Si7414DN striptape showing total-ionizing dose (TID) related discrete increases in I_D as individual Ar ions strike the DUT at the location of the gate oxide.

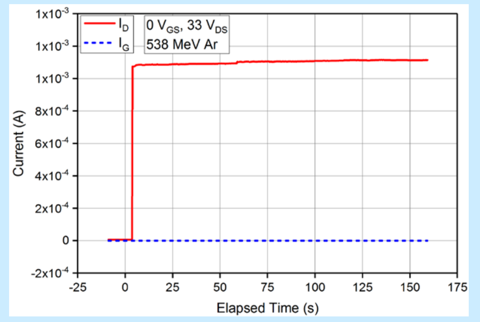

Fig. 12. Si7414DN striptape showing SEB event shortly after Ar beam shutter opened. Bias: 0 V_{GS} and 33 V_{DS}.

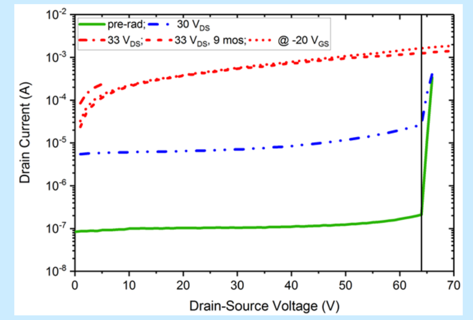

Fig. 13. Si7414DN BV_{DSS} curves pre-rad, after exposure in Fig. 11, and both immediately after SEB event in Fig. 12 & 9 months later. BV_{DSS} repeated at -20 V_{GS} confirms the effect is not TID related.

The localized flatband voltage shift is greater with 538-MeV Ar irradiation at -10 V_{GS} than at 0 V_{GS} (**Fig. 14**). Ion species (LET) impacts the $V_{GS(TH)}$ shift (**Fig. 15**), and heavy-ion localized dosing also increases I_{DSS} even when V_{GS} and V_{DS} are grounded (**Fig. 16**).

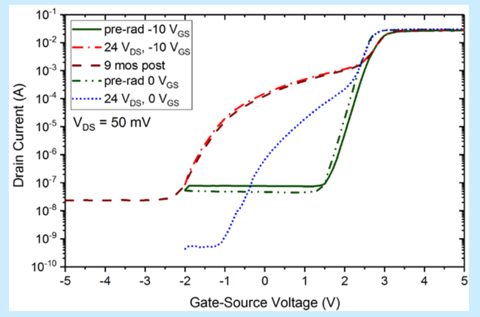

Fig. 14. Si7414DN I_D-V_{GS} curves for 2 DUTs irradiated with 3×10⁶ cm⁻² 538-MeV Ar: one at -10 V_{GS}, 24 V_{DS} and the other at 0 V_{GS} and 24 V_{DS}. Pre-rad curves in green.

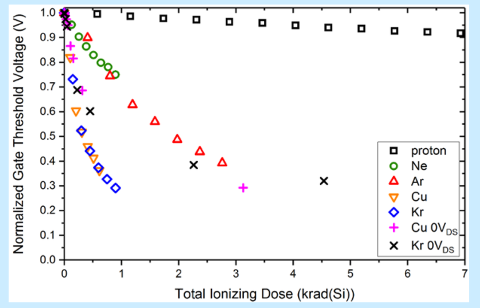

Fig. 15. Si7414DN normalized $V_{GS(TH)}$ vs. TID from protons or heavy ions. Bias: 0 V_{GS}; initial V_{DS} = 24 V with 3 V steps after each exposure, except 2 DUTs held at 0 V_{DS} (+ and × symbols).

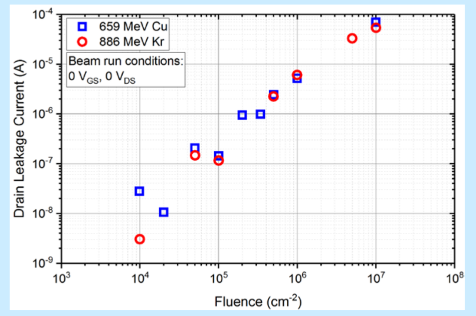

Fig. 16. Si7414DN I_{DSS} vs. Cu or Kr fluence for DUTs held at 0 V_{GS} and 0 V_{DS}.

Results: P-Type Automotive

Single-event gate rupture (SEGR) occurred in all 3 p-type trench-gate power MOSFETs under 886 MeV Kr irradiation (LET = 31 MeV·cm²/mg), but not under 659-MeV Cu (LET = 21 MeV·cm²/mg). **Figs. 17 – 19** show individual DUT threshold V_{DS} for SEGR at 0 V_{GS}. Square markers indicate the highest passing V_{DS}; error bars extend to the V_{DS} at which SEGR occurred. In **Fig. 19**, SEGR occurred on the first beam run for one DUT as indicated by the "X" marker. Most samples failed during the beam run, with SEGR occurring between the gate and drain.

Localized dosing of the gate oxide in p-type MOSFETs does not impact the function of the device because the positive $V_{GS(TH)}$ shift of the localized area is undetectable due to the overall lower $V_{GS(TH)}$.

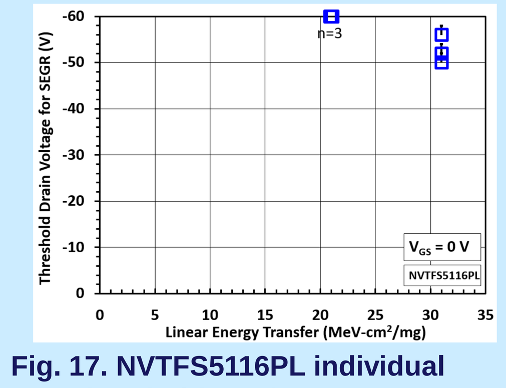

Fig. 17. NVTFS5116PL individual DUT threshold V_{DS} for SEGR at 0 V_{GS}.

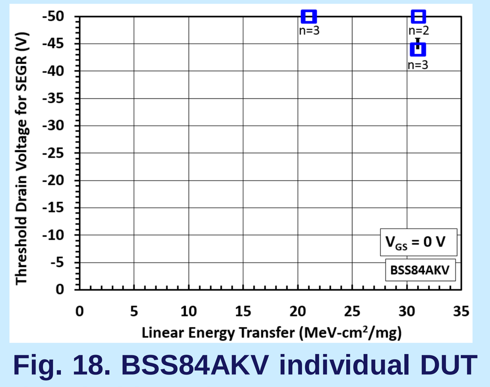

Fig. 18. BSS84AKV individual DUT threshold V_{DS} for SEGR at 0 V_{GS}.

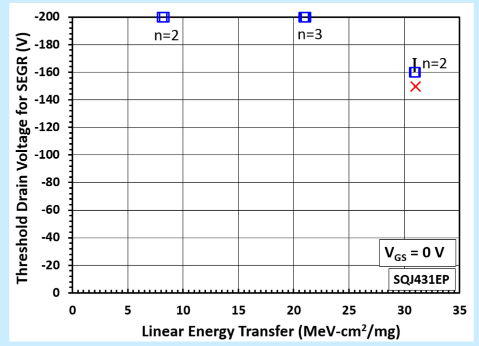

Fig. 19. SQJ431EP individual DUT threshold V_{DS} for SEGR at 0 V_{GS}.

Results: N-Type Rad-Hardened

The IRHLF87Y20 generation R8 20-V n-type MOSFET manufacturer SEE test data were validated (**Fig. 20**). Both SEGR and SEB occurred when irradiated with 1039 MeV Ag (LET = 48 MeV·cm²/mg) (**Figs. 21 – 23**). In contrast with commercial/automotive grade devices, there were no measurable total ionizing dose effects.

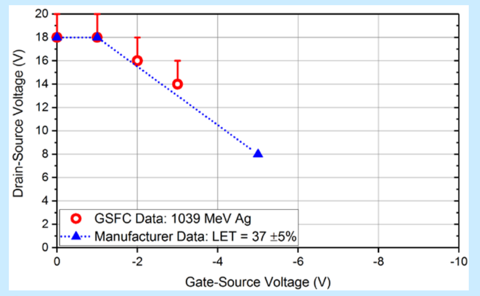

Fig. 20. IRHLF87Y20 SEE response curve: each marker = 3 samples.

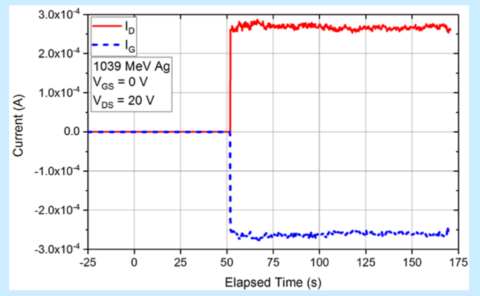

Fig. 21. Striptape showing SEGR at 0 V_{GS}, 20 V_{DS}.

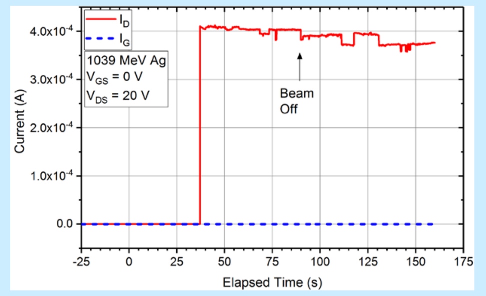

Fig. 22. Striptape showing SEB at 0 V_{GS}, 20 V_{DS}.

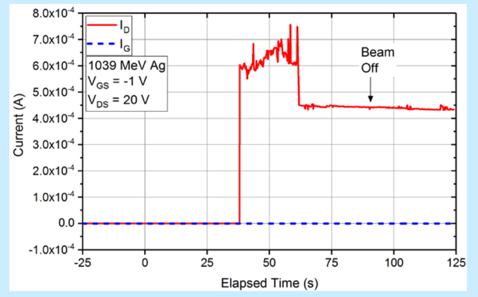

Fig. 23. Striptape showing SEB with spontaneous partial recovery.

Discussion & Conclusions

Commercial, automotive, and radiation-hardened trench-gate vertical power MOSFETs were evaluated for SEE sensitivity. The SEE safe operating area for the commercial and automotive-grade devices is difficult to define due to the extent of the part-to-part variability. In some cases, a bimodal distribution may be present. A standard radiation hardness assurance procedure is to apply a derating factor (typically 0.75, per [10]) to the highest passing V_{DS} of the sample that failed at the lowest V_{DS}. This approach is likely inadequate given the extent of the part-to-part variability. For example, a 0.75 derating factor applied to the data in **Fig. 17** suggests NVTFS5116PL can be operated safely up to a V_{DS} of 37.5 V; however, application of a 99/90 one-sided tolerance limit (KTL) to these data results in 30 V, indicating a larger sample size is needed to determine the distribution of failures.

Hardness assurance is further complicated by the localized dosing effects in the unhardened n-type trench-gate power MOSFETs. As shown in **Fig. 14**, the use of a hard-off V_{GS} bias to counter-act gate threshold voltage shift can increase the amount of shift for a given dose. As demonstrated in **Figs. 15-16**, flight spares having all nodes grounded degrade with heavy-ion fluence.

This study verified the manufacturer SEE response curve for the rad-hardened IRHLF87Y20. Importantly, no localized dosing effects were measured. The device exhibited three different failure signatures during irradiation, demonstrating greater complexity of failure mechanisms than those of planar-gate vertical power MOSFETs.

Acknowledgment

This work was supported in part by the NASA Electronic Parts and Packaging Program (NEPP), the NASA Engineering Safety Center (NESC), and International Rectifier Corporation (now Infineon, A.G).

In addition, we thank Michael Campola for his work on this project, Jim Forney and Stephen Cox for their technical assistance, and Rocky Koga, The Aerospace Corp., for scheduling LBNL beam time for these tests.

References

[1] J. A. Felix, *et al.*, "Enhanced degradation in power MOSFET devices due to heavy ion irradiation," *IEEE TNS,* vol. 54, Dec 2007.
[2] F. K. Galloway, "A brief review of heavy-ion radiation degradation and failure of silicon UMOS power transistors," *Electronics,* vol. 3, 2014.
[3] S. Kuboyama, *et al.*, "Characterization of microdose damage caused by single heavy ion observed in trench type power MOSFETs," *IEEE TNS,* vol. 57, 2010.
[4] S. Liu, *et al.*, "Vulnerable Trench power MOSFETs under heavy ion irradiation," presented at the IEEE NSREC, Tucson, AZ, USA, 14–18 July 2008.
[5] M. R. Shaneyfelt, *et al.*, "Enhanced proton and neutron induced degradation and its impact on hardness assurance testing," *IEEE TNS,* vol. 55, 2008.
[6] G. I. Zebrev, *et al.*, "Microdose induced drain leakage effects in power trench MOSFETs: Experiment and modeling," *IEEE TNS,* vol. 61, 2014.
[7] X. Wan, *et al.*, "Charge deposition model for investigating SE-microdose effect in trench power MOSFETs," *J. Semiconductors,* vol. 36, 2015.
[8] J. S. George, *et al.*, "Response variability in commercial MOSFET SEE qualification," *IEEE TNS,* vol. 64, 2017.
[9] MIL-STD-750-1A, "Test methods for semiconductor devices," ed: USDOD, Aug, 2016.
[10] K. Sahu, "EEE-INST-002: Instructions for EEE parts selection, screening, qualification, and derating," NASA/TP-2003-212242, 2003.

To be presented by Jean-Marie Lauenstein at the 2017 Institute of Electrical and Electronics Engineers (IEEE) Nuclear and Space Radiation Effects Conference (NSREC), NewOrleans, Louisiana, July 21, 2017.